



---

# Improving NCS Stabilization Using a Predictive Pulsed Control Law

O. Castillo, H. Benítez-Pérez

## Oriol Castillo\*

Instituto de Investigaciones en Matemáticas Aplicadas y en Sistemas  
Universidad Nacional Autónoma de México  
C.P. 04510, Coyoacán, Ciudad de México, México.

\*Corresponding author: [octavio.castillo@iimas.unam.mx](mailto:octavio.castillo@iimas.unam.mx)

## Héctor Benítez-Pérez

Instituto de Investigaciones en Matemáticas Aplicadas y en Sistemas  
Universidad Nacional Autónoma de México  
C.P. 04510, Coyoacán, Ciudad de México, México.

### Abstract

The aim in this paper is experimentally to show that a predictive *pulsed control law* is able to enlarge the stabilizing sampling periods of a networked control system (NCS) more than the classical predictive ZOH-control law. Additionally, using a comparison in the system response between the predictive pulsed control law and the predictive ZOH-control law, it is obtained that the pulsed control law requires less energy consumption to stabilize a NCS exposed to large time-delays. A 3-DOF Hover is used as case study.

**Keywords:** networked control systems, digital control, Bayesian prediction.

## 1 Introduction

Ideal control systems assume that flow of information is a continuous signal within a control loop. However, whenever a control system is physically implemented, the flow of information becomes a discontinuous signal due to presence both of the digital devices and the digital signal processing time. Special case happens as a control system is implemented over a digital communication network, case in that systems are called *networked control system* (NCS). In that case, digital devices and digital communication networks can provide flexibility, modularity, and low cost to control system implementation. However, this digital processing can also induce significant discontinuities in the flow of information; of course, the discontinuities arise from *lags* during the information update. If update is fast enough, then the discontinuous flow of information seems a continuous signal and the system performance is not affected. Conversely, if lags increase then the system performance degrades or even the system stability can be lost.

Two issues born here related to control theory: 1) the stability analysis of NCS, and 2) the search of control strategies to deal with time-delays on NCS. On one hand, stability analysis has been performed by three main approaches: the discrete approach, the time-delay system approach, and the

impulsive system approach. Discrete approaches are the earliest and can be found for example in [7]. The time-delay systems analysis can be found in [5, 6, 15]. And an impulsive system approach can be found in [13, 14]. On the other hand, different to stability analysis, some control strategies have appeared to deal with the loss of performance caused by large time-delays. These control strategies not only propose an stability analysis but also improve the control systems performance. Within these strategies, the most popular are predictive control techniques whose objective is to generate a set of time-ahead control predictions to use as *sampling* as time-delays become large. Examples of predictive control strategies can be found in [1, 9, 12, 19]. Otherwise, in the same line of control strategies, there is a little known strategy called *the pulsed control law* which has shown to improve the performance and even recover the stability of control systems exposed to large time-delays. Different from the standard way of applying the control law as a zero-order-hold (ZOH), where control signal is maintained constant between sampling times, the pulsed control law consists of maintaining the control signal constant for some period of time and then put in back till the next sampling time. In general, the novelty of the pulsed control law relies on the enlargement of the *stabilizing sampling period region* of the NCS without the need of redesigning a new control law. This result has been reported in [2, 3, 10, 11, 17], and a dynamic proof and explanation about this phenomenon is presented in [4].

It should be stressed that the ZOH-control law has played a major role in predictive strategies. In a different way, in this work the power both of a predictive strategy and a pulsed control law are merged to improve the NCS performance under a proposed configuration. The NCS configuration used in this paper consists of adding a predictor in the control loop and send one-step ahead predictions to the controller for computing the control algorithm. Once the control law packet reach the actuators, one can decide if the pulsed control law or the ZOH-control law is applied. To these ways of applying the control law to the system, we have called them the *predictive pulsed control law* or the *predictive ZOH-control law* respectively. Our intention in this paper is to compare the system response between the *predictive pulsed control law* and the *predictive ZOH-control law* as long as the NCS is exposed to random large time-delays. Two results are obtained: 1) it is shown that the *predictive pulsed control law* is able to preserve the NCS stability for larger time-delays more than the *predictive ZOH-control law*, and 2) for large sampling periods the predictive pulsed control law requires less energy consumption than the ZOH-control law for the NCS stabilization.

Outline of the paper is as follows. Section 2 describes details and assumptions of the proposed NCS reconfiguration, and a complete system model is obtained. In Section 3, the stability of the complete system model is discussed. In Section 4, the model of a 3-DOF Hover is introduced, and in Section 5 the comparison of the system response between the predictive pulsed control law and the predictive ZOH-control law is presented. Finally, conclusions are said in Section 6.

**Notation.** We use  $k$  to denote the time-stamp of packets considering that  $k \in \mathbb{Z}^+$  and  $\{k\}$  is an ordered sequence. Identity matrix in  $\mathbb{R}^{n \times n}$  is denoted by  $I$ .  $P > 0$  denotes a symmetric and positive definite matrix  $P \in \mathbb{R}^{n \times n}$ . Symbol “ $'$ ” stands for matrix transposition.  $N(\chi|\bar{\chi}, P)$  denotes a normal probability function of the random variable  $\chi$ , with mean  $\bar{\chi}$  and covariance matrix  $P$ .

## 2 System description

The block diagram of the used NCS configuration is shown in Figure 1. This configuration considers a continuous plant and assumes that samples are sent from the sampler as a packet with a time-stamp  $k$ . Also, a predictor has been added after sampler with the aim of sending state predictions through the network. Indeed, it is intended that the predictor compensates the effects of the network-time-delay over the control system.

Two relevant times arise within the control loop: 1) *the sampling instant*  $s_k$  where sensors pick up measurements of the output system, and 2) *the update control instant*  $t_k$  where the control signal is updated due to stamped packet  $k$ . Some standard definitions are derived from these instants. Namely, the *sampling period*  $T_k$  is defined as

$$T_k = s_{k+1} - s_k, \quad \forall k, \quad (1)$$

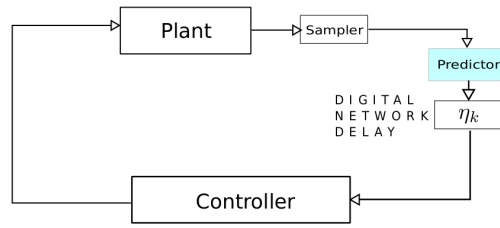


Figure 1: NCS with a predictor.

the *network-delay* is defined as

$$\eta_k = t_k - s_k, \quad \forall k, \tag{2}$$

and the *time-delay* is defined by

$$\tau(t) = t - s_k, \quad t_k \leq t < t_{k+1}. \tag{3}$$

Under previous definitions, a linear system with constant matrices  $(A, B)$  is described by

$$\dot{x}(t) = Ax(t) + Bu(t), \quad t_k \leq t < t_{k+1}, \tag{4}$$

where  $u(t)$  is the control law. Usually,  $u(t)$  is an algorithm based on measurements  $x(s_k)$  taken from the sampler. However, under configuration in Figure 1,  $u(t)$  is based on the predictor output. Thus, the predictor output was denoted as  $\hat{x}(s_k + \eta_k)$  to emphasize that its output is an estimate of the state  $x$  after  $\eta_k$ -seconds ahead to the sampling time  $s_k$ . In consequence, for a given state feedback matrix  $K$ , the control law given by

$$u(t) = K\hat{x}(s_k + \eta_k), \quad t_k \leq t < t_{k+1}, \tag{5}$$

is defined as the *predictive ZOH-control law*, and the control law given by

$$u(t) = \begin{cases} K\hat{x}(s_k + \eta_k), & \text{if } t_k \leq t < t_k + h, \\ 0, & \text{if } t_k + h \leq t < t_{k+1}, \end{cases} \tag{6}$$

is defined as the *predictive pulsed control law* for  $0 < h < (t_{k+1} - t_k)$ . Thus, our aim in the following is to compare both control laws (5) and (6) as long as network-delays  $\eta_k$  becomes larges and the stabilizing state feedback matrix  $K$  is the same.

## 2.1 Assumptions

In general, in NCS the communication channels are not perfect and the flow of information is always exposed to random time-delays and packet losses. However, in order to deal with the randomness of the network-delay, it is assumed that the following three assumptions hold:

**Assumption 1.** *The state feedback matrix  $K$  asymptotically stabilizes the system (4) without time-delays, i.e. the matrix  $A + BK$  is a Hurwitz matrix.*

**Assumption 2** (Gaussian randomness). *The network-delay  $\eta_k$  is considered to be an uncorrelated random variable with an statistical behavior described by*

$$\eta_k \sim N(\eta_k | \bar{\eta}, \sigma^2)$$

where  $N(\eta_k | \bar{\eta}, \sigma^2)$  denotes a normal probability function with mean  $\bar{\eta}$  and covariance  $\sigma^2$ .

**Assumption 3** (Zero packet losses). *There are no packet losses in the network, and the sampling instant  $s_{k+1}$  is triggered by the control update instant  $t_k$ , i.e.*

$$s_{k+1} = t_k \quad \forall k. \tag{7}$$

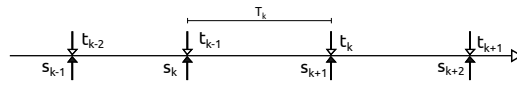


Figure 2: Sampling periods are equal to the network-delays by Assumption 3.

**Remark 2.1.** It must be stressed that Assumption 3 implies that  $\eta_k = T_k$  for every  $k$ , i.e. the  $k$ -th network-delay is equal to the  $k$ -th sampling period (see Figure 2). Furthermore, notice that  $\eta_k = T_k$  does not imply neither  $T_k = T_{k+1}$  nor  $\eta_k = \eta_{k+1}$  for every  $k$ . Later could be only possible in probability sense due to the statistical behavior of  $\eta_k$  (Assumption 2). Therefore, by Assumption 3 we have that

$$\sup_{t_k \leq t < t_{k+1}} \tau(t) = T_k + \eta_{k+1} = T_k + T_{k+1}. \tag{8}$$

This is the maximum time-delay experienced by the system (4).

## 2.2 Modelling

In order to implement and get a complete model of the NCS with the configuration in Figure 1, both an appropriate system model and a prediction model are needed. Notice that two complete models must exist, one for the predictive ZOH-control law and other one for the predictive pulsed control law. Assumptions 1-3 were used to deduce these models.

### 2.2.1 The system model

Let  $\bar{\eta} = T$  be the mean sampling period of the random variable  $\eta_k$ . Hence, thanks to Assumption 3, we can solve the differential equation (4) for the mean sampling period  $T$  at times  $t_k$  to get the discrete model

$$\begin{cases} x(k+1) = \bar{A}x(k) + \bar{B}_\sigma u(k) + q(k) \\ y(k) = Cx(k) + r(k), \end{cases} \tag{9}$$

where  $q(k)$  and  $r(k)$  are additive, uncorrelated and zero-mean noise quantities generated by the  $\eta(k)$ -randomness and sensor measurements respectively such that

$$q(k) \sim N(q(k)|0, Q), \quad r(k) \sim N(r(k)|0, R). \tag{10}$$

Notice that  $q(k)$  represents the uncertainty at solving the differential equation (4) because of the presence of the digital network.

A code variable  $\sigma$  was added to distinguish between the system model generated by the control law used: fixing  $\sigma = 1$  denotes the solution to the system (4) using the predictive ZOH-control law (5), and fixing  $\sigma = 2$  denotes the solution to the system (4) using the predictive pulsed control law (6). Namely,

$$\bar{A} = e^{AT}, \quad \bar{B}_1 = \int_0^T e^{As} ds, \quad \bar{B}_2 = \int_0^h e^{A(T-s)} ds, \quad C = I. \tag{11}$$

### 2.2.2 Prediction model

To build the prediction model, it was used the Bayesian approach addressed in [18] to predict the one-step-ahead state of the system  $\hat{x}(k+1)$  at time-step  $k$ . Under this approach, three models are needed: the probabilistic system model  $p(x(k+1)|x(k))$ , the probabilistic measurement model  $p(y(k)|x(k))$ , and the solution to the Kolmogorov equation

$$p(x(k+1)|y(k)) = \int p(x(k+1)|x(k))p(x(k)|y(k))dx(k). \tag{12}$$

From (9) and (10), we have that

$$p(x(k+1)|x(k)) = N(x(k+1)|\bar{A}x(k) + \bar{B}_\sigma u(k), Q), \tag{13}$$

$$p(y(k)|x(k)) = N(y(k)|Cx(k), R). \tag{14}$$

Hence, by [18], using (13) and (14), the solution to (12) at every  $k$ -step, is given by a recursive computation of *update* and *prediction*. *Update* is given by

$$p(x(k)|y(k)) = N(x(k)|\hat{x}^+(k), P_k^+)$$

with

$$\hat{x}^+(k) = \hat{x}(k) + P_k C'(C P_k C' + R)^{-1}(y(k) - C\hat{x}(k)) \tag{15}$$

$$P_k^+ = P_k - P_k C'(C P_k C' + R)^{-1} C P_k, \tag{16}$$

and prediction is given by

$$\begin{aligned} p(x(k+1)|y(k)) &= \int p(x(k+1)|x(k))p(x(k)|y(k))dx(k) \\ &= N(x(k+1)|\hat{x}(k+1), P_{k+1}) \end{aligned} \tag{17}$$

where

$$\hat{x}(k+1) = \bar{A}\hat{x}^+(k) + \bar{B}_\sigma u(k) \tag{18}$$

$$P_{k+1} = \bar{A}P_k^+ \bar{A}' + Q. \tag{19}$$

Equations (15)-(16) and (18)-(19) form jointly the prediction model.

### 2.2.3 The complete system model

Defining

$$F_k = P_k C'(C P_k C' + R)^{-1},$$

and replacing (15) in (18), we get that the predicted state is given by

$$\hat{x}(k+1) = (\bar{A} - \bar{A}F_k C)\hat{x}(k) + \bar{B}_\sigma u(k) + \bar{A}F_k y(k). \tag{20}$$

Then, using (20) and the system model (9), we have that the *prediction error* defined as  $\tilde{x}(k+1) = x(k+1) - \hat{x}(k+1)$  is given by

$$\tilde{x}(k+1) = (\bar{A} - \bar{A}F_k C)\tilde{x}(k) - \bar{A}F_k r(k) + q(k). \tag{21}$$

On the other hand, the system model can be rewritten as

$$\begin{aligned} x(k+1) &= \bar{A}x(k) + \bar{B}_\sigma(K\hat{x}(k) - Kx(k) + Kx(k)) + q(k) \\ &= (\bar{A} + \bar{B}_\sigma K)x(k) - \bar{B}_\sigma K\tilde{x}(k) + q(k). \end{aligned} \tag{22}$$

Hence, using (21) and (22), the complete system model results in

$$\begin{bmatrix} x(k+1) \\ \tilde{x}(k+1) \end{bmatrix} = \begin{bmatrix} \bar{A} + \bar{B}_\sigma K & -\bar{B}_\sigma K \\ 0 & \bar{A} - \bar{A}F_k C \end{bmatrix} \begin{bmatrix} x(k) \\ \tilde{x}(k) \end{bmatrix} + \begin{bmatrix} q(k) \\ q(k) - \bar{A}F_k r(k) \end{bmatrix}. \tag{23}$$

Previous model is the complete system model related to the NCS in Figure 1. Recall that  $\sigma$  stands for the control law used, the predictive ZOH-control law ( $\sigma = 1$ ) or the predictive pulsed control law ( $\sigma = 2$ ).

## 3 Stability

To analyze the stability of the model (23), notice that if we take its expected value, then by the *separation principle*, the system stability is guaranteed iff  $(\bar{A} + \bar{B}_\sigma K)$  and  $(\bar{A} - \bar{A}F_k C)$  are *Schur* matrices. This type of stability is commonly known as *stability in mean* []. Thus, for getting *stability in mean* we have to ensure that  $(\bar{A} + \bar{B}_\sigma K)$  and  $(\bar{A} - \bar{A}F_k C)$  are Schur matrices. We focus on these

points. On one hand, since we are assuming that  $(A + BK)$  is a Hurwitz matrix (Assumption 1), then the matrix  $(\bar{A} + \bar{B}_\sigma K)$  must be *Schur* for small sampling periods  $T$ . On the other hand, the *Schur* property of  $(\bar{A} - \bar{A}F_k C)$  is guaranteed if the covariance matrix  $P_k$  converges to some matrix  $P > 0$ . To study this convergence, it is replaced (16) in (19) for getting

$$P_{k+1} = \bar{A}P_k\bar{A}' - \bar{A}P_kC'(CP_kC' + R)^{-1}CP_k\bar{A}' + Q. \tag{24}$$

Previous equation is the *recursive Riccati equation*, and it is known to be convergent to  $P > 0$  as  $k \rightarrow \infty$  if either of the following conditions holds

- (i) The pair  $(A, C)$  is observable provided  $R > 0$  [8].
- (ii) The pair  $(A, C)$  is detectable and the pair  $(A, Q^{\frac{1}{2}})$  is stabilizable [16].

Thus whereas either of the later requirements hold, the matrix  $\bar{A} - \bar{A}F_k C$  will be *Schur*.

Summarizing, we can establish the following

- Small sampling periods  $T$  ensures  $\bar{A} + \bar{B}K$  is Schur.
- Either condition (i) or condition (ii) ensures  $\bar{A} - \bar{A}F_k C$  is Schur.

In the following, specially in testing, we select matrices  $A, B, K, C, R$  such that the Schur property of the matrices  $\bar{A} + \bar{B}K$  and  $\bar{A} - \bar{A}F_k C$  is guaranteed for small sampling periods.

## 4 Case study

To achieve our goals, a 3-DOF Hover system distributed by Quanser company was used as case study (see Figure 3). In general, the dynamic of this system is non-linear, however if the Hover is operated under certain conditions, then the Hover dynamic can be considered as linear.



Figure 3: Quanser 3-DOF Hover.

The built-in controller provided by Quanser allows us to regulate the system orientation by controlling the *yaw* ( $\psi$ ), *pitch* ( $\theta$ ), and *roll* ( $\phi$ ) angles of the Hover. The linear dynamic is achieved by regulating the  $\psi$ -position under  $\theta = \phi = 0$ . Thus, under  $\theta = \phi = 0$ , the continuous system model is

$$\begin{cases} \dot{x}(t) = Ax(t) + Bu(t) \\ y(t) = Cx(t) \end{cases} \tag{25}$$

where  $x(t) = [\psi \ \theta \ \phi \ \dot{\psi} \ \dot{\theta} \ \dot{\phi}]'$ , and

$$\begin{aligned}
 A &= \begin{bmatrix} 0 & 0 & 0 & 1 & 0 & 0 \\ 0 & 0 & 0 & 0 & 1 & 0 \\ 0 & 0 & 0 & 0 & 0 & 1 \\ 0 & 0 & 0 & -0.0001 & 0 & 0 \\ 0 & 0 & 0 & 0 & -0.0002 & 0 \\ 0 & 0 & 0 & 0 & 0 & -0.0002 \end{bmatrix}, \\
 B &= \begin{bmatrix} 0 & 0 & 0 & 0 & 0 \\ 0 & 0 & 0 & 0 & 0 \\ 0 & 0 & 0 & 0 & 0 \\ -0.0326 & -0.0326 & 0.0326 & 0.0326 \\ 0.4235 & -0.4235 & 0 & 0 \\ 0 & 0 & 0.4235 & -0.4235 \end{bmatrix}, \\
 K &= - \begin{bmatrix} -55.90 & 66.14 & 0.00 & -20.70 & 18.11 & 0.00 \\ -55.90 & -66.14 & -0.00 & -20.70 & -18.11 & -0.00 \\ 55.90 & 0.00 & 66.14 & 20.70 & 0.00 & 18.11 \\ 55.90 & -0.00 & -66.14 & 20.70 & -0.00 & -18.11 \end{bmatrix} \\
 C &= I.
 \end{aligned}$$

Now, from previous matrices and for a fixed value of  $T$ , the complete system model (23) is obtained by computing the system model (9) and the prediction model given by equations (15)-(16) and (18)-(19).

Hence, using the matrices  $(A, B, C)$  of the 3-DOF Hover, the system model (9) is formed by computing the matrices  $\bar{A}$  and  $\bar{B}_\sigma$  through (11), and the prediction model is formed using the previous matrices  $\bar{A}, \bar{B}_\sigma, C$  and the following covariance matrices

$$\begin{aligned}
 Q &= \begin{bmatrix} 0.01 & 0 & 0 & 0 & 0 & 0 \\ 0 & 0.01 & 0 & 0 & 0 & 0 \\ 0 & 0 & 0.01 & 0 & 0 & 0 \\ 0 & 0 & 0 & 0.01 & 0 & 0 \\ 0 & 0 & 0 & 0 & 0.01 & 0 \\ 0 & 0 & 0 & 0 & 0 & 0.01 \end{bmatrix} \\
 R &= \begin{bmatrix} 0.289 & 0 & 0 & 0 & 0 & 0 \\ 0 & 0.289 & 0 & 0 & 0 & 0 \\ 0 & 0 & 0.289 & 0 & 0 & 0 \\ 0 & 0 & 0 & 0.029 & 0 & 0 \\ 0 & 0 & 0 & 0 & 0.029 & 0 \\ 0 & 0 & 0 & 0 & 0 & 0.029 \end{bmatrix} \times 10^{-6} \\
 P_0 &= I.
 \end{aligned} \tag{26}$$

It is stressed that there are two complete system models, one induced by the predictive ZOH-control law ( $\sigma = 1$ ) and other one induced by the predictive pulsed control law ( $\sigma = 2$ ). Our task in the next section, is to compare the system response between these models ( $\sigma = 1$  and  $\sigma = 2$ ) as the mean sampling period  $\bar{\eta} = T$  increases.

**Remark 4.1.** From the matrices in (25) and (26), hand calculations show that  $A + BK$  is a Hurwitz matrix,  $Q$  and  $R$  are positive definite matrices, and the pair  $(A, C)$  is observable. As a result, the matrices  $\bar{A} + \bar{B}_k K$  and  $\bar{A} - \bar{A} F_k C$  are Schur matrices and then the 3-DOF Hover under configuration in Figure 1 must be stable for small sampling periods.

## 5 Results

The tests consisted of setting up the 3-DOF Hover as in Figure 1, and compare the system performance between the predictive ZOH-control law (5) and the predictive pulsed control law (6). As

performance measures, we select the standard energy of the error signal (ESE) and the control signal energy (CSE) defined as

$$ESE = \int_0^t e'(s)e(s)ds$$

with  $e(t) = x(t) - x_q$ , where  $x_q$  is the desired equilibrium point, and

$$CSE = \int_0^t u'(s)u(s)ds. \tag{27}$$

Our control routine consisted of switching the desired equilibrium point  $x_q$  between two positions,  $x_{q1} = [000000]'$  and  $x_{q2} = [30^\circ 00000]'$ , and compare the measures of ESE and CSE as the predictive pulsed control law or the predictive ZOH-control law is used. This routine was repeated for several mean sampling periods, namely  $T = 10[ms]$ ,  $20[ms]$ ,  $40[ms]$ ,  $60[ms]$ ,  $100[ms]$ .

For getting a comparison of the system response between the predictive ZOH-control law and the predictive pulsed control law, we have plot the system state  $x$ , the predicted state  $\hat{x}$ , and the measures of ESE and CSE for each control law: Figure 4 shows the results obtained by using the *predictive ZOH-control law* and Figure 5 shows the results obtained by using the *predictive pulsed control law* for a mean sampling period  $T = 40[ms]$ . Figure 6 and 7 show the results using the *predictive ZOH-control law* and the *pulsed control law* respectively, as the mean sampling period is  $T = 60[ms]$ . Finally, the same routine under  $T = 100[ms]$  was done; Figures 8 and 9 show its results.

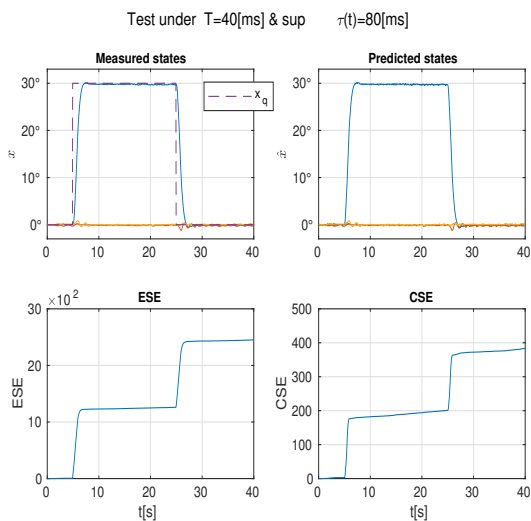


Figure 4: Test under the *predictive ZOH-control law* and  $T = 40[ms]$ .

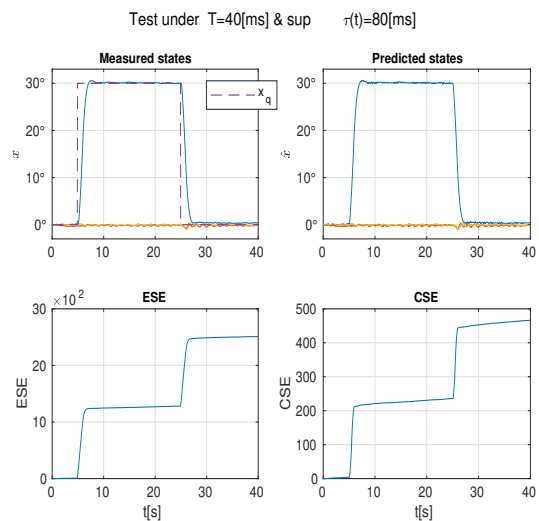


Figure 5: Test under the *predictive pulsed control law* and  $T = 40[ms]$ .

During previous testing, it was observed that the *predictive ZOH-control law* preserves the system stability only as the sampling period  $T$  is in the region  $0 \leq T < 60[ms]$ . On the other hand, as Figure 9 shows, the *predictive pulsed control law* remains the system stability for sampling periods  $T$  greater than  $60[ms]$ , actually until  $T = 100[ms]$ . For summarizing results, Table 1 collects the maximum values of ESE and CSE for each sampling period  $T$  and control law used. Figure 10 depicts these maximum ESE's as a function of the sampling periods  $T$  for each control law. From Figure 10, we see that for small sampling periods, the predictive pulsed control law requires more energy than the predictive ZOH control law to stabilize the NCS. However, as sampling period  $T$  increases, the energy consumption is larger using the predictive ZOH control law than using the pulsed control law. Even, the predictive pulsed control law maintains the NCS stability for larger sampling periods than the predictive ZOH-control law as Figures 8 and 9 depict.

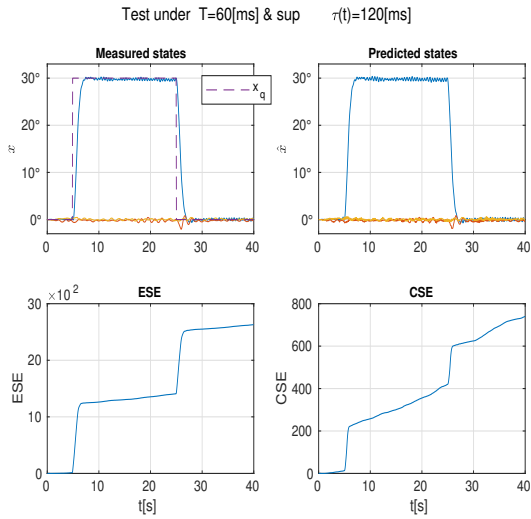


Figure 6: Test under the *predictive ZOH-control law* and  $T = 60[ms]$ .

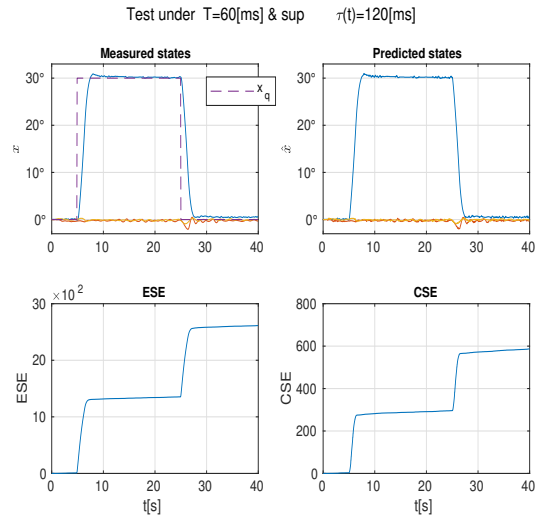


Figure 7: Test under the *predictive pulsed control law* and  $T = 60[ms]$ .

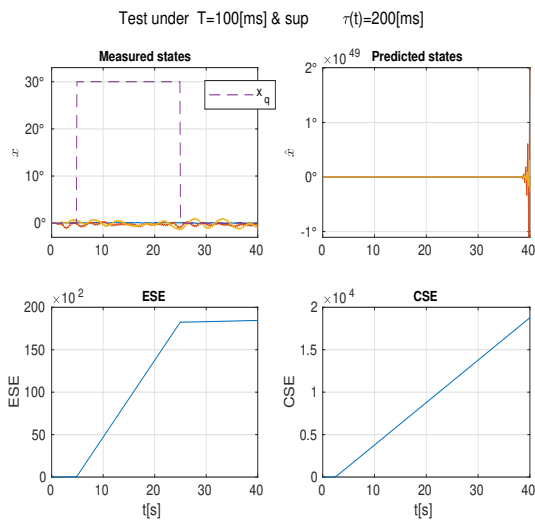


Figure 8: Test under the *predictive ZOH-control law* and  $T = 100[ms]$ . The systems is unstable.

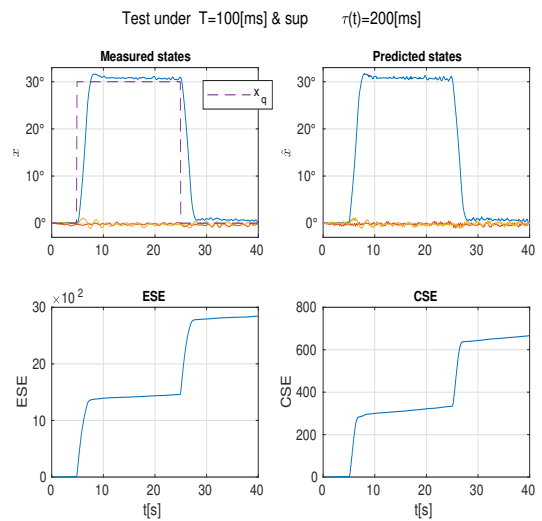


Figure 9: Test under the *predictive pulsed control law* and  $T = 100[ms]$ .

Table 1: ESE and CSE comparison between the *predictive ZOH-control law* and the *predictive pulsed control law*.

	$T = 10[ms]$		$T = 20[ms]$		$T = 40[ms]$		$T = 60[ms]$		$T = 100[ms]$	
	ZOH	Pulsed	ZOH	Pulsed	ZOH	Pulsed	ZOH	Pulsed	ZOH	Pulsed
ESE	2461.6	-	2449.1	-	2451.1	2510.4	2630.7	2613.4	-	2844.1
CSE	351.12	-	348.68	-	383.43	466.13	740.06	587.00	-	666.65

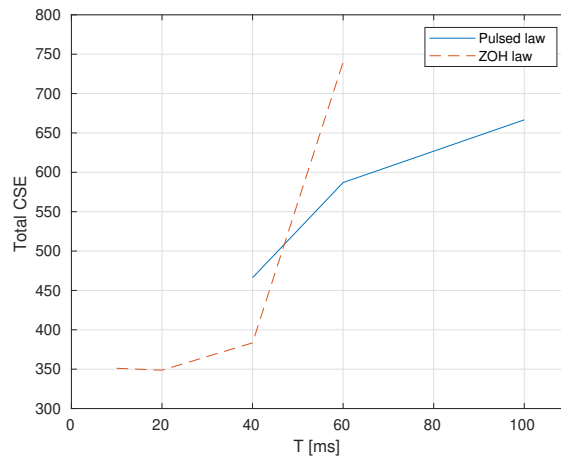


Figure 10: *Total energy consumptions for both the predictive pulsed control law and the predictive ZOH-control law.*

## 6 Conclusions

Previous works related to the pulsed control law have reported that the stabilizing sampling period region of NCS is enlarged as it is used. This paper has shown that the *pulsed control law* keeps its effectiveness even if random network-delays are present in the control loop, and this control law works fine along with the classical theory about bayesian predictors.

Furthermore, one interesting result in the paper is that for large sampling periods, referring us to the system energy consumption, the system stabilization using the pulsed control law is not as hard as using the ZOH-control law. In this sense, our results can be summarized saying that the ZOH-control law is convenient as sampling is small, but the pulsed control law is more convenient as sampling is large. The reasons of later is because of the following reasons: 1) whenever there are large time-delays, the pulsed control law stabilizes the system to a lower energy cost than the ZOH-control law, and 2) the pulsed control law is able to preserve the system stability for larger time-delays than the ZOH-control law. Previous results can be so useful in NCS where control systems are exposed to large time-delays. For instead, if a communication network is not busy, the *predictive ZOH-control law* can be used, but if there is congestion or a fault in communication channels and time-delays becomes large, then the *predictive pulsed control law* can be applied with better benefits than the predictive ZOH-control law.

Finally, it is worth of mention that a strong assumption in our work is the *zero packet losses* in communication channels. Rarely communication networks exhibit zero packet losses. However, there are communication protocols (particularly protocols focused on automation control systems as *Profibus*) which guarantee that every message reach its destiny performing retransmissions to ensure reliable messaging as TCP/IP. This enables our work.

## Funding

This work was supported by Project PAPIIT IT100320 by National Autonomous University of México (UNAM), and CONACYT México.

## Author contributions

The authors contributed equally to this work.

## Conflict of interest

The authors declare no conflict of interest.

## References

- [1] Beldiman, O.; Walsh, G. C. Bushnell, L. (2000). Predictors for networked control systems. In *Proceedings of the 2000 American Control Conference. ACC (IEEE Cat. No. 00CH36334)*, v4, 2347–2351, 2000.
- [2] Briat, C. (2014). Spectral necessary and sufficient conditions for sampling-period-independent stabilisation of periodic and aperiodic sampled-data systems using a class of generalised sampled-data hold functions. *International Journal of Control*, 87(3), 612–621, 2014.
- [3] Castillo, O.; Benítez-Pérez, H. (2017). A novel technique to enlarge the maximum allowable delay bound in sampled-data systems. In *Congreso Nacional de Control Automático 2017*, Monterrey, Nuevo León, México. Asociación Mexicana de Control Automático, 2017.
- [4] Castillo, O.; Benítez-Pérez, H.; Alvarez-Icaza, L. (2020). Novel analysis of sampled-data systems stabilised by a pulsed control signal. *International Journal of Control*, 0(0):1–9.
- [5] Fridman, E. (2010). A refined input delay approach to sampled-data control. *Automatica*, 46(2):421–427.
- [6] Fridman, E. (2014). *Introduction to time-delay systems: Analysis and control*. Springer.
- [7] Halevi, Y.; Ray, A. (1988). Integrated communication and control systems: Part i—analysis.
- [8] Kalman, R. E. (1960). A new approach to linear filtering and prediction problems. *Transactions of the ASME—Journal of Basic Engineering*, 82(Series D):35–45.
- [9] Li, H.; Sun, Z.; Liu, H.; Chow, M.-Y. (2008). Predictive observer-based control for networked control systems with network-induced delay and packet dropout. *Asian journal of control*, 10(6):638–650.
- [10] Li, X.-G.; Cela, A.; Niculescu, S.-I.; Reama, A. (2009a). A switched control method for networked control systems. *IFAC Proceedings Volumes*, 42(14):61–65.
- [11] Li, X.-G.; Niculescu, S.-I.; Reama, A., et al. (2009b). Stability analysis of networked control systems based on a switched control. *IFAC Proceedings Volumes*, 42(20):358–363.
- [12] Liu, B.; Xia, Y.; Mahmoud, M. S.; Wu, H.; Cui, S. (2012). New predictive control scheme for networked control systems. *Circuits, Systems, and Signal Processing*, 31(3):945–960.
- [13] Naghshtabrizi, P.; Hespanha, J. P.; Teel, A. R. (2008). Exponential stability of impulsive systems with application to uncertain sampled-data systems. *Systems & Control Letters*, 57(5):378–385.
- [14] Naghshtabrizi, P.; Hespanha, J. P.; Teel, A. R. (2010). Stability of delay impulsive systems with application to networked control systems. *Transactions of the Institute of Measurement and Control*, 32(5):511–528.
- [15] Seuret, A. (2012). A novel stability analysis of linear systems under asynchronous samplings. *Automatica*, 48(1):177–182.
- [16] Su, J.; Li, B.; Chen, W.-H. (2015). On existence, optimality and asymptotic stability of the kalman filter with partially observed inputs. *Automatica*, 53, 149–154, 2015.
- [17] Sun, X.-M.; Liu, G.-P.; Rees, D.; Wang, W. (2008). A novel method of stability analysis for networked control systems. *IFAC Proceedings Volumes*, 41(2), 4852–4856, 2008.
- [18] Särkkä, S. (2013). *Bayesian Filtering and Smoothing*. Institute of Mathematical Statistics Textbooks. Cambridge University Press, 2013.
- [19] Zheng, Y.; Fang, H.; Wang, Y. (2004). Kalman filter based fdi of networked control system. In *Fifth World Congress on Intelligent Control and Automation (IEEE Cat. No. 04EX788)*, IEEE, 2, 1330–1333, 2004.



Copyright ©2020 by the authors. Licensee Agora University, Oradea, Romania.

This is an open access article distributed under the terms and conditions of the Creative Commons Attribution-NonCommercial 4.0 International License.

Journal's webpage: <http://univagora.ro/jour/index.php/ijccc/>



This journal is a member of, and subscribes to the principles of,  
the Committee on Publication Ethics (COPE).

<https://publicationethics.org/members/international-journal-computers-communications-and-control>

*Cite this paper as:*

Castillo, O.; Benítez-Pérez, H. (2020). Improving NCS Stabilization Using a Predictive Pulsed Control Law, *International Journal of Computers Communications & Control*, 15(6), 4052, 2020.

<https://doi.org/10.15837/ijccc.2020.6.4052>.